Theoretical Spectroscopy of Astaxanthin in Crustacyanin Proteins: Absorption, Circular Dichroism, and Nuclear Magnetic Resonance

ARTICLE *in* THE JOURNAL OF PHYSICAL CHEMISTRY B · MARCH 2011

Impact Factor: 3.3 · DOI: 10.1021/jp111579u · Source: PubMed

3 AUTHORS, INCLUDING:

Francesco Buda
Leiden University
102 PUBLICATIONS **2,879** CITATIONS

SEE PROFILE

THE JOURNAL OF PHYSICAL CHEMISTRY B

ARTICLE

pubs.acs.org/JPCB

Theoretical Spectroscopy of Astaxanthin in Crustacyanin Proteins: Absorption, Circular Dichroism, and Nuclear Magnetic Resonance

Johannes Neugebauer,* Jan Veldstra, and Francesco Buda*

Gorlaeus Laboratories, Leiden Institute of Chemistry, Leiden University, P.O. Box 9502, 2300 RA Leiden, The Netherlands

Supporting Information

ABSTRACT: The bathochromic shift (>0.5 eV) in the absorption spectrum of the carotenoid astaxanthin upon incorporation into crustacyanin proteins is investigated. Several previously suggested explanations are tested and assessed by direct comparison to experimental absorption and circular dichroism spectra. We investigate the effect of extended models for the protein binding pocket, which results in only small contributions to the total shift. The possible explanation in terms of protonated histidine residues interacting with the astaxanthin molecules is analyzed by calculation of nuclear magnetic resonance chemical shifts. The results indicate that such a protonation is unlikely. In addition, we show that excitonic couplings are too weak to explain the red shift in the absorption spectrum, but the resulting intensity distribution actually leads to a blue shift of the major absorption peak. These findings are corroborated by a comparison of the theoretical and experimental circular dichroism spectra. We analyze changes in the relative orientation of the two astaxanthin molecules present in β-crustacyanin, which may lead to increased excitonic coupling and modified intensity distributions.

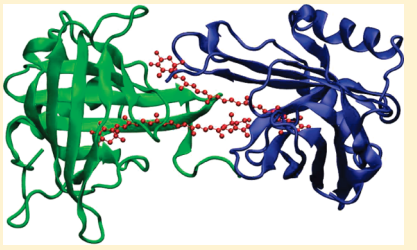

1. INTRODUCTION

The carotenoid molecule astaxanthin (AXT) in crustacyanin proteins, which occur in the shell of the lobster *Hommarus gammarus*, has a dark blue color, which changes to the bright red color of the free astaxanthin when exposed to heat[1] due to denaturation of the protein. Two forms of protein−pigment complexes are observed, namely, β-crustacyanin (see Figure 1), a dimer of 1:1 AXT−protein complexes, and α-crustacyanins, which are octamers of β-crustacyanins and thus contain 16 AXT molecules. The absorption maxima of the lowest energy absorption band, corresponding to the $S_0 \rightarrow S_2$ transition,[2] are ∼630 nm (1.97 eV) in α-crustacyanin and ∼580−590 nm (2.10−2.14 eV) in β-crustacyanin; the absorption maximum of astaxanthin as a free molecule in solution is solvent dependent and appears at a wavelength between 472 (2.63 eV, *n*-hexane) and 506 nm (2.45 eV, CS_2); an overview including many other solvents is given in ref 3.

The coloration mechanism of the crustacyanin proteins has been the subject of many theoretical and experimental studies in the past, and findings have been summarized recently by Strambi and Durbeej.[4] Essentially, three factors have been identified that could be responsible for the shift in the absorption maximum: (i) conformational changes between solution and protein-bound structure, (ii) polarization effects due to the protein environment, which depend crucially on the protonation state of nearby histidine residues, and (iii) exciton coupling effects.

Although conformational effects apparently do lead to a red shift in the absorption due to an extended delocalization of the π system, there seems to be an agreement that they are only of the order of 0.1 eV[1,5,6] and thus can only explain a minor part of the total shift, which is about 0.50 eV for β-crustacyanin and about 0.65 eV for α-crustacyanin relative to *n*-hexane solution. A debate is going on about the importance of the latter two effects, which can be summarized as follows: Buchwald and Jencks[7] invoked excitonic effects to explain certain spectroscopic features of aggregates of astaxanthin molecules, in particular concerning structures in the circular dichroism (CD) and optical rotatory dispersion (ORD) spectra. They also conclude, however, that a single type of excitonic splitting cannot explain both the small splitting in the ORD spectrum and the large shift of the absorption wavelength in the aggregates of pigments investigated in their study. There is clear evidence that excitonic interactions play a role in the CD spectrum of crustacyanins, which lead to a couplet-like sign change at 610 (β-crustacyanin) or 630 nm (α-crustacyanin).[8] Very similar CD signatures were observed for intrinsically nonchiral carotenoid molecules like canthaxanthin, in which the hydroxyl groups of astaxanthin are replaced by hydrogen atoms.[8] This further supports the importance of exciton couplings for the CD spectra of crustacyanins, although not necessarily for the spectral shift. A calculation based on a transition−dipole interaction model for the astaxanthin dimer in the orientation as present in the β-crustacyanin crystal structure (PDB code 1GKA[9]) resulted in an exciton coupling constant (V_{12}) of 0.49 eV, which suggested that exciton splitting would be the dominant mechanism for the bathochromic shift.[1] Further evidence for the importance of exciton couplings was provided by a time-resolved absorption study, which revealed that there is also a large red shift in the $S_1 \rightarrow S_n$ transition energies, which are

Received: December 6, 2010
Revised: January 31, 2011
Published: March 10, 2011

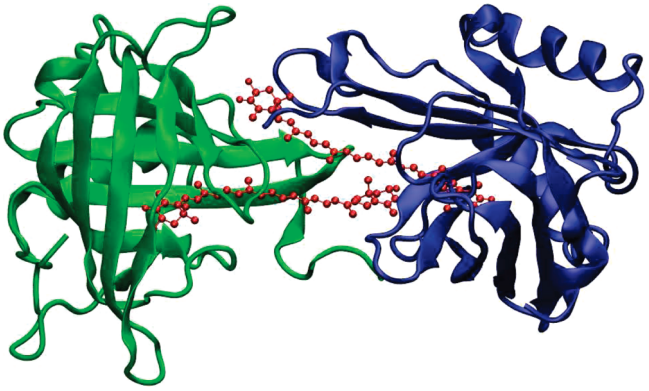

Figure 1. AXT dimer in β-crustacyanin. The structure was taken from PDB crystal structure with code 1GKA (graphics: VMD[60]).

also strongly allowed and thus may be sensitive to excitonic couplings.[2] However, recent work by Strambi and Durbeej based on quantum chemical dimer calculations showed that the transition−dipole interaction overestimates the coupling in the dimer considerably.[4] On the basis of their calculations, they estimated the exciton splitting to be on the order of 0.08 eV for the β-crustacyanin geometry of the dimer, which would correspond to a contribution to the shift of only about 0.04 eV. These results are almost independent of the type of electronic-structure method used. There are other observations that cast some doubt on the importance of exciton effects for the spectral shift. For example, it has been reported that a similar bathochromic shift is observed for the protein asteriarubin, which contains only one carotenoid molecule and no exciton interaction.[8,10] A recent study on the blue carotenoid violerythrin shows that specific structural features lead to a blue neutral carotenoid without invoking excitonic interactions.[11] Furthermore, the CD spectrum of α-crustacyanin after heating still exhibits the exciton coupling, although the couplet shows a spectral shift similar to the absorption spectrum.[8]

Strambi and Durbeej[4] instead propose that polarization effects due to the protein environment play a major role. In particular, a strong hydrogen-bonding interaction with nearby protonated histidine residues, as reported in earlier computational studies,[6,12] is mentioned. This is in line with the spectral changes observed when treating astaxanthin or related molecules with strong acids, leading to blue products identified as oxonium ions (see ref 13 and references therein as well as the early study in ref 3). Evidence for the polarization mechanism comes from resonance Raman[14] as well as nuclear magnetic resonance (NMR) studies.[8] The latter report significant downfield shifts in the ^{13}C NMR signals for C(14) and C(14′) as well as for C(12) and C(12′), which would be consistent with protonated carbonyl groups at C(4) and C(4′) according to theoretical considerations.[8] However, even larger effects were expected for C(6) and C(6′) and for C(8) and C(8′) according to these considerations and according to experimental data for protonated canthaxanthin.[13] A subsequent NMR study found, however, only a minor effect on the NMR signals for these atoms, leading to the conclusion that no large charge effect can play a role.[1]

As far as the computational methods are concerned, Durbeej and Eriksson demonstrated that the semiempirical ZINDO/S method is well suited to reproduce the absorption maxima of both AXT and the protonated form AXTH$^+$ (single protonation at one keto group).[6,12] Configuration-interaction singles (CIS) calculations give excitation energies to the ^{1}B$_u$-like state that are too large by about 0.5−0.7 eV for AXT and AXTH$^+$, but the error appears to be systematic. This is in contrast to B3LYP time-dependent density functional theory (TDDFT) excitation energies, which are in quite good agreement with experiment for AXTH$^+$, but underestimate the experimental value by roughly 0.4−0.5 eV for AXT. They are therefore not well suited for changes in excitation energies due to charge polarization effects. The spectral shift induced by protonation of AXT was thus found to be about 1.1 eV for ZINDO/S, 1.0 eV for CIS, and 0.5 eV for B3LYP, compared to 1.06 eV in experiment. Note that problems for spectral shifts induced by charged residues in the environment are also reported for retinal proteins in ref 15. In that case, the situation is somewhat different because the charged group carries a negative charge and the excitation involved has a partial charge-transfer character. Neither CIS nor TDDFT methods are considered accurate in that study, and both considerably underestimate the spectral shift. The study in ref 12 further reported the influence of several amino acids found in the AXT binding pockets. The largest change (−0.67 eV) was observed for a protonated histidine residue bound to one keto group together with a water molecule bound to the other one. The neutral histidine in combination with the water, however, resulted only in a minor change of −0.03 eV.

The purpose of the present manuscript is 2-fold. First, we investigate specific effects within the protein binding site, employing larger models than those used in previous studies. In this way, it shall be clarified whether the combined effect of the residues in the protein binding site can explain a significant part of the spectral shift without the assumption of protonated histidine residues, which are apparently not in line with NMR data. Chemical shift calculations are presented to directly assess the validity of this assumption. In a second step, we reinvestigate the exciton coupling effects and elucidate their consequences for absorption and circular dichroism spectra, i.e., not only the energetics of the exciton coupling but also the effects on the intensities in absorption and CD spectra will be investigated. In addition, geometrical and electronic factors, which could influence the exciton splitting, will be investigated. In contrast to former studies, we will consider not only the peak positions in electronic spectra but also the intensity distribution.

2. COMPUTATIONAL DETAILS

Density functional calculations were carried out with the ADF program package.[16,17] If not mentioned otherwise, geometry optimizations and NMR chemical shift calculations were performed with the Becke−Perdew (BP86) functional[18,19] and a TZP basis set. For excitation-energy calculations, we employ standard basis sets (DZP, TZP, TZ2P) from the ADF basis-set library in connection with the statistical averaging of (model) orbital potentials (SAOP) potential,[20−22] which is well suited for molecular response properties. These calculations are augmented with ADF calculations employing the M06-HF functional,[23] featuring 100% exact exchange, and with BLYP,[24] B3LYP,[25,26] configuration-interaction singles (CIS), and time-dependent Hartree−Fock (TDHF, or random phase approximation, RPA) calculations using the program package Turbomole.[27] Additional semiempirical ZINDO/S[28] calculations were performed with the program ORCA.[29]

For investigation of exciton couplings, we also performed subsystem TDDFT calculations[30,31] with a development version

of ADF. For the ground-state subsystem DFT (or frozen-density embedding, FDE) calculations,[32,33] we employed the nonadditive kinetic-energy functional called GGA97.[34,35] This functional makes use of the PW91 kinetic-energy functional, which has the same functional form for the enhancement factor $F(s)$ as the exchange functional of Perdew and Wang[36] and was parametrized for the kinetic energy by Lembarki and Chermette.[37] The exchange-correlation component of the embedding potential is evaluated with the same exchange-correlation functional that is used for the nonembedding part. In the case of the orbital-dependent SAOP potential, we use the potential derived from the Becke exchange-energy functional[18] and the Perdew−Wang correlation functional.[36] The adiabatic local density approximation (ALDA) was employed for the exchange-correlation kernel in ADF TDDFT calculations. In subsystem TDDFT calculations, this also applies to the kinetic-energy component of the response kernel, for which the Thomas−Fermi kinetic-energy functional[38,39] is used.

In FDE ground-state calculations, the subsystem densities were relaxed in three freeze−thaw cycles[40] to include the mutual polarization of the monomer densities. From the resulting orbitals and orbital energies, we calculated local excitations within the uncoupled FDE (FDEu) approximation[41] in the terminology introduced in refs 30 and 31. These calculations include the effect of the other monomer on the potential in the DFT calculation[41] but not its response. Subsequent subsystem TDDFT or coupled FDE (FDEc) calculations[30,31] were performed in which the lowest 10 excitations per monomer were coupled.

Usually, we consider the excitation energy of the lowest B_u-like excitation with the dominant HOMO → LUMO contribution of AXT for calculation of the spectral shifts. For several models, this orbital transition spreads over two or more excited states and the associated intensity is distributed over several states. Therefore, we also compare the maximum absorption energies E_{max} obtained as the maxima of the bands in the absorption spectra, which are represented as a superposition of Gaussian peaks with an integral equal to the oscillator strength of the transition and a half-width of 0.3 eV. This provides a more direct measure for the spectral shift observed in experiment. All excited states up to 2.0 eV are considered in these superpositions.

It is well known that TDDFT is problematic for linear-polyene-type molecules, in particular for the excited states with significant double-excitation character.[42−47] For the bright low-lying B_u-like state of linear polyenes that we investigate here, however, the double-excitation character is low[45] and typically rather good results can be obtained[47] (for a comparison of DFT and approximate coupled cluster methods for excited-state potential energy surfaces, see ref 48). Nevertheless, we carried out some tests to assess the accuracy that can be expected from the SAOP potential. A comparison of excitation energies obtained with SAOP/TZP for small all-trans linear polyenes (C_{2h} symmetry) to theoretical best estimates (TBEs) and experimental data is shown in Figure 2. It can clearly be seen that SAOP produces the experimental trend for the excitation energies quite well, albeit the absolute excitation energies are underestimated. The offset increases a bit for longer polyenes, but similar problems are also observed for the TBEs and the additional data shown from spin-flip (SF) TDDFT[49−51] using the local density approximation (LDA) and the Tamm−Dancoff approximation (TDA). The latter method incorporates also doubly substituted determinants, since it effectively generates singly substituted determinants from the lowest triplet state, and is thus better suited to describe excitations with partial double-excitation character.[47,51]

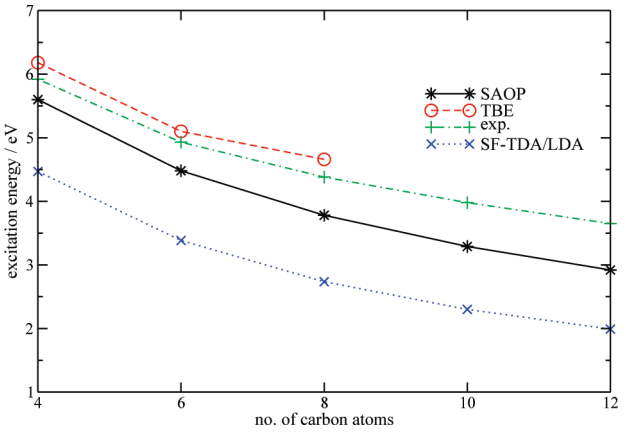

Figure 2. Excitation energies (SAOP/TZP, SF-LDA-TDA/TZP, and theoretical best estimates (TBEs, from ref 61)] of the lowest ^1B_u states of all-trans linear polyenes as a function of the number of carbon atoms. Shown are experimental data (taken from ref 62 for butadiene and hexatriene and from the compilation of estimated gas-phase data in ref 63 for octatetraene, decapentaene, and dodecahexaene).

Table 1. Lowest B_u-like Excitation Energies E_{ex} and Oscillator Strengths f of Several Models for Free Astanxanthin, AXT1, and AXT2 from β-Crustacyanin[a]

model	E_{ex}/eV	f	E_{max}/eV
s-cis-AXT	1.655	3.78	1.655
s-trans-AXT	1.619	4.04	1.619
AXT1	1.576	4.35	1.576
AXT1 + hydrophil. residues, N(1)−H	1.557	3.47	1.545
AXT1 + hydrophil. residues, N(3)−H	1.537	1.72	1.538
AXT2	1.546	4.23	1.548
AXT2 + hydrophilic residues, N(3)−H	1.495	4.05	1.493

[a] E_{max} indicates the maximum absorption energy in the simulated spectra (see Computational Details). In AXT1 and AXT2 structures, only the positions of the hydrogen atoms have been optimized.

3. ON-SITE EFFECTS

We start our investigation on the possible origins of the bathochromic shift of astaxanthin in crustacyanins with a study of local (on-site) effects. Among the on-site effects we can distinguish the structural change from the *s-cis*-AXT to the *s-trans*-AXT and changes in the site energies of the astaxanthin molecules due to the binding pocket.

To analyze the former point, we fully optimized both structures (BP86/TZP/small core); they are shown in Figure S1 in the Supporting Information. In addition, we considered the *s-trans*-AXT1 and -AXT2 structures as obtained from crystal structure analysis. Hydrogen atoms have been added to that structure, and their positions have been optimized while keeping all heavy atoms fixed. In addition, we considered all hydrophilic residues in the binding pockets of AXT1 and AXT2, respectively, to set up minimal models for the astaxanthins in their binding pockets. For these models, all heavy atoms involved in hydrogen bonding were optimized while all other heavy atom positions

Table 2. Effect of Inclusion or Removal of a Specific Amino Acid to the AXT1-Binding Pocket (bp) Model on the Excitation Energies E_{ex} (in units of eV) of the Lowest B_u-Like State[a]

residue	E_{ex} (AXT1 + residue)	E_{ex} (AXT1 + bp − residue)
Asn-54	1.570	1.556
Gln-37	1.574	1.564
Gln-46	1.573	1.555
Tyr-56	1.574	1.560
Tyr-97	1.569	1.567
Ser-67	1.575	1.563
His-90	1.576	1.552
water-2973	1.574	1.560
(none)	1.576	1.557

[a] His-90 is protonated at N(1) in these calculations.

Table 3. Effect of Inclusion or Removal of a Specific Amino Acid to the AXT2-Binding Pocket (bp) Model on the Excitation Energies E_{ex} (in eV) of the Lowest B_u-Like State[a]

residue	E_{ex} (AXT2 + residue)	E_{ex} (AXT2 + bp − residue)
Asn-86	1.541	1.496
Asp-123	1.544	1.497
Gln-32	1.542	1.498
Gln-41	1.545	1.505
Glu-90	1.544	1.498
His-92	1.542	1.520
Ser-49	1.545	1.497
Ser-94	1.541	1.498
Thr-64	1.538	1.504
Tyr-51	1.539	1.495
water-2013	1.546	1.496
water-2019	1.543	1.499
(none)	1.546	1.495

[a] His-92 is protonated at N(3) in these calculations.

were kept fixed. The excitation energies for all of these structures are shown in Table 1. We note that the effect of using a frozen core during structure optimization is very small. In the subsequent excitation calculations, in which no frozen core is used, we obtained a difference of about 0.001 eV when using a structure optimized without a frozen core.

The difference in excitation energy between the optimized *s-cis* and optimized *s-trans* form is found to be 0.036 eV. The change in energy between the free *s-cis* structure in solution and the structure in β-crustacyanin is −0.079 eV for AXT1 and −0.109 eV for AXT2, which is in good agreement with the shift of −0.08 eV reported in ref 1. As a next step, we included all hydrophilic residues in the immediate surroundings of AXT1. This leads to a further decrease of 0.019 eV if protonation at N(1) [N^{π}] is assumed for His-90 and of 0.039 eV if protonation at N(3) [N^{τ}] is assumed. The latter protonation pattern is preferrable for the formation of a hydrogen bond to the keto group. However, no optimum hydrogen-bonding situation is obtained here due to the restriction on the position of the heavy atoms not directly involved in hydrogen bonding, so that the optimum orientation of the histidine relative to AXT1 cannot be reached. The same holds for AXT2, where we find an additional decrease due to the hydrophilic residues, including His-92 protonated at N(3), of 0.051 eV. The effect is thus slightly larger than that for AXT1, which could have a simple structural reason due to a better orientation of His-92 relative to AXT2. This will be further investigated below. However, when considered individually, most other amino acids in the binding pocket lower the excitation energy by an amount comparable to the histidine residue, for both AXT1 and AXT2. A difference between the effect of the histidine residues and the other amino acids that we could observe in our calculations is that the histidines lead to a more pronounced distribution of the intensity over two or more electronic transitions.

The change in the excitation energy caused by the hydrophilic residues of the binding pocket is rather modest, suggesting that none of the amino acids has a large effect. In ref 1 it was reported that the change in excitation energy due to histidine and a water molecule (at the other keto group) in an optimized geometry was about 0.07 eV. This is on the same order of magnitude as the entire effect that we observe here with nonoptimized hydrogen-bonding geometries but including the other hydrophilic residues. In order to analyze what the influence of the individual residues is, we carried out four series of calculations, two for each AXT in β-crustacyanin. In series 1 and 3, we added a single residue from the binding pocket to AXT1 and AXT2, respectively, while in series 2 and 4 we considered all but one residue. The results are shown in Tables 2 and 3. Note that in the AXT1 case protonation of His-90 at N(1) was assumed, whereas we considered protonation at N(3) in the case of His-92 for AXT2. The effect of changing to the other (probably more likely) tautomer for AXT1 can be estimated from the data given in Table 1. As can be seen from the data in Tables 1 and 2, none of the residues in the binding pockets has a strong effect on the absorption energy.

When looking at the data in Table 3, it seems that adding the His-92 residue to the bare chromophore induces a red shift of only 0.004 eV, whereas removing the same residue from the chromophore plus binding pocket model actually increases the excitation energy by a much larger value of 0.025 eV. The latter value is in good agreement with the effect of the neutral histidine residue found by Durbeej and Eriksson[12] (0.03 eV) but seems to be inconsistent with the first value. A problem here is that another state acquires significant intensity in our calculation. If we determine the maximum of the absorption peak according to the procedure outlined in section 2, then adding the histidine residue to the bare chromophore leads to a red shift of 0.010 eV and removing the residue from the binding pocket gives a consistent blue shift of 0.014 eV. This also indicates that care has to be taken when looking at shifts in excitation energies only.

As a next step, we investigated the changes in the excitation energy upon protonation of the histidine residues. The results can be found in Table 4. Analysis is complicated even more here by the fact that the HOMO → LUMO orbital transition, which gives rise to high intensity, is distributed over several excitations for the protonated species. Because of this distribution of the orbital transition (and the associated intensity), the best way to determine the spectral shift is probably not to look at the changes in the excitation energies of the lowest intense transition, which may overestimate the spectral shift. Instead, it appears necessary to try to model the absorption spectrum directly and to determine the absorption maximum from that simulation.

Nevertheless, an upper bound for the protonation-induced spectral shift may be obtained by looking at the change in excitation energy for the lowest transition with considerable

Table 4. Lowest B_u-Like Excitation Energies (E_{ex}; SAOP/TZP) of Several Models of AXT1 and AXT2 from β-Crustacyanin Including a (model for) a Protonated Histidine Residue[a]

model	E_{ex}/eV (f)	E_{max}/eV
s-cis-AXT	1.655 (3.78)	1.655
s-trans-AXT	1.619 (4.04)	1.619
AXT1 + hydrophilic residues, N(1)−H, N(3)−H	1.418, 1.573, 1.583 (1.64, 1.57, 1.48)	1.535
AXT1 + His-90, N(1)−H, N(3)−H	1.434, 1.583, 1.597 (1.30, 1.05, 2.22)	1.561
AXT1 + imidazole−H^+, partial optimization (**1a**)	1.438, 1.595 (1.46, 3.10)	1.557
AXT1 + imidazole−H^+, full optimization (**1b**)	1.377, 1.629 (1.60, 3.02)	1.604
AXT2 + hydrophilic residues, N(1)−H, N(3)−H	1.392, 1.511 (1.38, 3.50)	1.482
AXT2 + His-92, N(1)−H, N(3)−H	1.378, 1.552 (1.38, 3.47)	1.527

[a] The positions of all hydrogen atoms and of all atoms directly involved in hydrogen bonding have been optimized. The results for the free AXT in fully optimized *s-cis* or *s-trans* structures (BP86/TZP/small core) are given for comparison. If no unambiguous assignment was possible, several excitation energies are listed. Oscillator strengths f are given in parentheses. Also listed are the maxima (E_{max}) of the spectral peaks simulated as described in the computational details.

HOMO → LUMO character. These are found at 1.418 and 1.434 eV for AXT1 with protonated His-90 (with and without inclusion of the other hydrophilic residues in the binding pocket, respectively) and at 1.392 and 1.378 for AXT2 with protonated His-92. This would correspond to an additional excitation energy lowering of about 0.1 eV compared to the AXT1/AXT2 models surrounded by the hydrophilic residues of their binding pocket with neutral histidines. The HOMO → LUMO orbital transition mixes heavily with two other $\pi \rightarrow \pi^*$ orbital transitions from HOMO−2 to LUMO and from HOMO to LUMO+1 of the AXT molecule. The HOMO−1 orbital of AXT is not a π-type orbital of the polyene chain but is located on one of the β-ionone rings. To summarize, we find that the maximum shift that can be calculated with our (partially relaxed) protonated histidine models relative to *s-cis*-AXT is −0.277 eV.

In order to see if additional structural relaxation would lead to a better hydrogen-bonding orientation and to a significant increase in the spectral shift, we replaced His-90 in the AXT1−His-90 complex by a protonated imidazole ring and carried out a partial optimization in which all hydrogen atoms and the entire imidazole ring were relaxed (model **1a**) and a full optimization in which also the entire AXT1 molecule was relaxed (model **1b**). Again, we observe a distribution of the intensity over two excited states; for both models, the higher-lying state carries most of the intensity. If we determine the shift based on the lowest state with considerable HOMO → LUMO character (**1a** 1.438 eV, **1b** 1.377 eV; shifts with respect to *s-cis* AXT **1a** −0.217 eV, **1b** −0.278 eV), we find values that are comparable to the one observed for AXT2 with protonated His-92. Calculations on the basis of the peak maxima reduce the shifts to 0.099 (**1a**) and 0.051 eV (**1b**). This indicates that His-92 in the crystal structure apparently shows a more favorable hydrogen-bonding orientation relative to AXT2 than is the case in the AXT1−His-90 pair.

In Table 4 we also list the absorption maxima determined from spectra plots as explained in section 2. When they are employed to determine the spectral shifts, the maximum change observed is 0.173 eV (for AXT2 including all hydrophilic residues and a protonated His-92). It is thus about 0.1 eV smaller than the largest shift based on the lowest B_u-like excitation energies.

Table 5. Lowest B_u-Like Excitation Energies (in eV) of AXT2 (model 2) and AXT2 with Protonated His-92 (model 3) from different Electronic-Structure Methods

method	model **2**	model **3**	shift
BLYP/TDA/TZVP	1.964	2.009	+0.044
B3LYP/TZVP	1.644	1.522	−0.122
M06-HF/TZP	1.480	1.312	−0.168
CIS/TZVP	2.285	2.160	−0.125
TDHF/TZVP	2.036	1.911	−0.126
ZINDO/S	1.833	1.594	−0.239

Considering the peak maximum in the spectrum leads to a less pronounced bathochromic shift prediction.

It could be argued that the splitting of the intensity to several peaks is an artifact of the TDDFT calculation. Even if the B_u state is described reasonably well, other states may be less well described so that an artificial mixing between different electronic transitions is introduced. If this was the case, the position of the absorption peak maximum, which in a sense averages over the intense subpeaks, may be the more reliable information to use for determination of the spectral shift. In order to shed more light on this question, we performed several other calculations on the free AXT2 molecule (**2**) and AXT2−His-92^+ (**3**). In this comparison, we include the BLYP/TDA approach that was found to predict good excitation energies for linear polyenes in ref 42, the hybrid functionals B3LYP and M06-HF, as well as CIS, TDHF, and ZINDO/S. CIS was shown to predict the shift between protonated and neutral AXT accurately in ref 12 even though the absolute excitation energies were significantly overestimated. The results from our calculations are shown in Table 5. BLYP/TDA calculations lead to a blue shift in the most intense peak, and again, the HOMO−LUMO transition is distributed over several excitations (the other ones lying at even higher energies). All other methods give a rather consistent picture of a red shift of about 0.12−0.17 eV with little intensity distribution. Only ZINDO/S predicts a more pronounced red shift of 0.239 eV. A reason for the larger shift found with ZINDO/S in ref 12 may

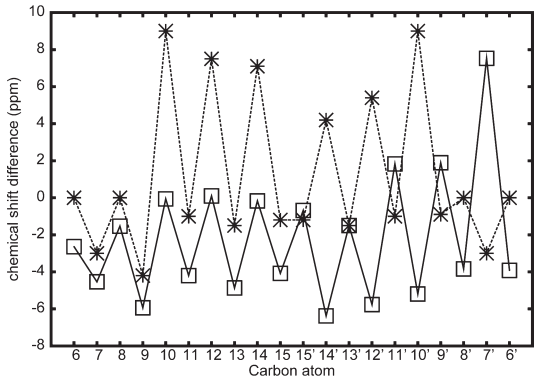

Figure 3. Experimental ^{13}C chemical shift difference between astaxanthin bound to α-crustacyanin and in solution (stars) compared to the computed chemical shift difference between the AXT2 + His-92$^+$ + water model and the isolated AXT2 model (squares). The experimental data are taken from ref 1. The lines are only a guide to the eyes.

be the different structure used there (optimized structure instead of the crystal structure used here). To check the effect of the structure, we additionally performed a constrained optimization of the AXT2 molecule (**2**) in which the bond lengths were optimized while keeping the bond angles and dihedral angles fixed. The ZINDO/S method for this partially optimized model gives an excitation energy of 2.077 eV to be compared with the ZINDO/S value of 2.193 eV for the optimized *s-cis*-AXT model and 2.117 eV for the optimized *s-trans*-AXT model. Therefore, the ZINDO/S method gives a shift of −0.116 eV for the conformational change, consistent with earlier works.

4. NMR CHEMICAL SHIFTS

In order to assess the validity of the hypothesis that a protonated histidine near the astaxanthin chromophore might contribute to the bathochromic shift, we show here a comparison between experimental NMR data and computed chemical shifts. We consider the model of an isolated astaxanthin (AXT2) and the same model with inclusion of a protonated histidine and a water molecule hydrogen bonded according to the X-ray data of β-crustacyanin (AXT2 + His-92$^+$ + water).

^{13}C NMR data of astaxanthin in solution and bound to α-crustacyanin were reported in ref 1. In Figure 3 we show the chemical shift difference between the data in the protein and the data in solution, which gives insight into the perturbation of the electronic charge of the chromophore upon binding to the protein. We can see that the perturbation due to binding is essentially symmetric with respect to the center of the chromophore: Only for C9/C9′, C12/C12′, and C14/C14′ are slightly different chemical shifts observed, probably due to a nonfully symmetrical protein environment.

In Figure 3 we compare the experimental data with the computed chemical shift difference between the AXT2 + His-92$^+$ + water model and the AXT2 model. The differences in the computed ^{13}C chemical shifts show a pattern along the conjugated carbon chain that is qualitatively different from the experimental one. Moreover, the presence of the protonated histidine induces a strong asymmetry between the two halves of the chromophore, contrary to the experimental finding: On the side where the water molecule is located (C6−C15) the perturbation is quite small and the behavior is qualitatively similar to the experiment, although there are quantitative differences. Instead, for the carbon atoms in the other half (C6′−C15′), where the protonated histidine is located, there is a qualitative mismatch with the experimental data. These results point against the assumption of a charged residue in close proximity of the chromophore. Yet, the origin of the perturbation due to the protein, which according to the experimental data is mainly localized in the center of the molecule (C10, C12, C14), remains to be clarified.

5. EXCITON COUPLINGS IN THE ASTAXANTHIN DIMER

To reinvestigate exciton coupling effects, we took the structure of the astaxanthin dimer (see Figure 4) from the Supporting Information of ref 4 without further modification. It was shown in that reference that exciton splittings obtained with SAOP agree well with those of other methods tested, including hybrid functionals, the semiempirical ZINDO/S method, and CIS calculations. Therefore, we will employ SAOP for all calculations presented in the following. To be able to distinguish mutual effects on the site energies of the two chromophores from exciton coupling effects, we performed both standard Kohn−Sham (TD)DFT calculations and subsystem TDDFT calculations.[30,31] The latter are also advantageous in terms of efficiency, so that basis-set and geometric effects can be analyzed more easily.

For the isolated astaxanthin monomers in the structure of the dimer we find two low-lying excitations with considerable intensity (data shown in Table 6). Both excitations are very close in energy (within less than 0.01 eV for both monomers) and show a heavy mixing of single-orbital transitions. To investigate the mutual interaction of the two monomers, we first performed an FDEu calculation, i.e., a calculation in which the effect of the other monomer is included in terms of an effective embedding potential, followed by a calculation on the local excitation energies of the chromophore considered as the active part. This calculation neglects exciton interactions between the two monomers, which can be evaluated separately in a second step.[52]

In the FDEu calculation, it can be seen that already the ground-state interaction of the monomers lifts the near-degeneracy a bit and leads to a splitting of about 0.03 eV between the two local excitations on each monomer. When excitonic coupling effects are considered, in terms of either a supermolecular calculation or using the FDEc formalism,[30,31] the dimer excitations show a splitting of 0.078 eV between the lowest and the highest excitation in this energy range. The FDEc results are in very good agreement with the supermolecular calculation: Differences of only about 0.003 eV are observed for the excitation energies, and the difference in the splitting energy is <0.001 eV. Also, oscillator and rotatory strengths are in very good agreement, as can be seen from the data in Table 6 as well as from the stick representation of the spectra in Figure 5. Note that supermolecular SAOP/DZP data have also been presented in ref 4, which we reproduce with our results here.

The splitting energies have been calculated on the basis of the FDEc approach also for larger basis sets. As can be seen from Table SI in the Supporting Information, the basis-set effect on the couplings is rather small, although larger basis sets in general increase the splitting slightly.

We observe that the exciton splitting in our calculations actually leads to a blue shift of the intense peak, whereas only the less intense peak is shifted to lower energies. This is in

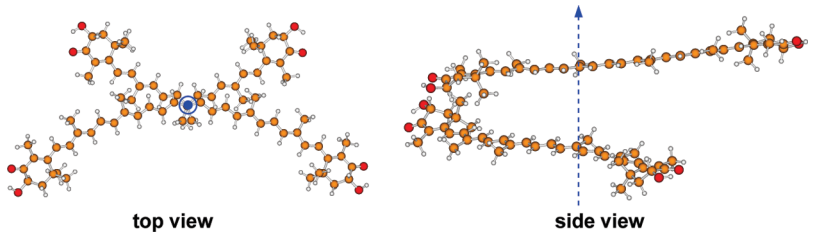

Figure 4. Structure of the astaxanthin dimer (coordinates taken from ref 4) and generation of displaced structures: Dimer structures with different orientations were obtained by rotating one monomer around the axis indicated in blue while keeping the other one fixed.

Table 6. Excitation Energies *E* (SAOP/DZP; in eV) and Oscillator Strengths *f* for the Astaxanthin Dimer[a]

	monomer 1				monomer 2			
	E_1	f_1	E_2	f_2	E_1	f_1	E_2	f_2
iso	1.691	2.72	1.699	0.79	1.691	2.63	1.693	0.87
FDEu	1.681	1.92	1.710	1.59	1.678	1.74	1.705	1.76
dimer excitations								
FDEc	1.651	0.79	1.690	0.59	1.701	0.18	1.729	5.14
super	1.648	0.78	1.689	0.68	1.700	0.18	1.726	5.07

[a] Shown are results from calculations of the isolated monomers (iso), a supermolecule calculation of the dimer (super), as well as uncoupled (FDEu) and coupled (FDEc) subsystem TDDFT calculations.

contrast to the experimentally observed shift of the entire absorption band to longer wavelengths (lower energies).[8] The exciton coupling effect not only is too small to explain the bathochromic shift of AXT in crustacyanins but also actually leads to an intensity shift in the wrong direction. Our findings are corroborated by a comparison of our circular dichroism spectra to the experimental one in ref 8. The experimental spectrum clearly shows a couplet-like structure, i.e., a negative peak at lower absorption energies (longer wavelengths, ~648 nm) and a positive peak at higher absorption energies (shorter wavelengths, ~554 nm). This is in line with our calculated rotational strengths. The difference in the peak maxima for the negative and positive peaks in the experimental spectrum corresponds to an energy of about 0.33 eV, which is considerably higher than the calculated exciton splitting. However, this could be caused by additional overlapping bands for the positive peak of the CD spectrum. This assumption is supported by two facts: (i) The absolute intensity is much higher for the positive than for the negative peak and (ii) the position of the positive peak in the CD spectrum is blue shifted compared to the absorption maximum. When assuming that the positive peak of the couplet should coincide with the maximum of the absorption spectrum (which is a rough guess because of possible broadening effects that can lead to a partial cancellation of positive and negative contributions in the CD spectrum), the energy difference to the negative peak in the experimental spectrum reduces to ~0.19 eV. This is much closer to the calculated splitting but still about a factor of 2 larger.

A possible reason for the mismatch may be that the orientation of the chromophores in the crystal structure sligthly differs from that in the protein under natural conditions. To estimate the effect of a change in the mutual orientation of the monomers in the dimer on the excitonic coupling, we varied the angle between the monomer chains by a rotation around the axis indicated in Figure 4. The resulting energy splittings (SAOP/TZP/FDEc) are shown in Figure 6. The splitting shows minima for rotations of about 40° (0.024 eV) and −130° (0.042) relative to the crystal structure orientation, whereas maxima are obtained for rotations of −50° (0.159 eV) and 130° (0.1881 eV). It can be seen that even small rotations by about −20° from the crystal structure orientation may increase the splitting energy by roughly 50%. Note that the amplitude of the curve changes between the different minima and maxima because the conjugated chain of the monomers is not exactly perpendicular to the chosen rotation axis, so that the minimum distance between the two monomers varies. The large changes in the splitting energy are accompanied by changes in the distribution of the intensity over the exciton states. To investigate the total effect on the spectrum, we modeled the absorption spectrum by applying a broadening of 0.3 eV to each peak. We then determined the maximum in the superposition of all peaks for different structures distorted around the conformation found in experiment. As can be seen from Figure S2 in the Supporting Information, the resulting peak maximum is always shifted to energies higher than the absorption energy of the uncoupled monomers, i.e., there is a blue shift.

We note that the crystals used to obtain the 1GKA crystal structure are of blue color, which indicates that differences in the inclination angle between the two astaxanthin molecules in β-crustacyanin cannot be used as an argument in favor of the exciton-coupling color tuning mechanism. This is not a contradiction to our calculations, which do not predict a bathochromic shift due to excitonic coupling at all. Nevertheless, a slight change in this angle could explain the mismatch between the calculated splittings and the splitting energies estimated from experimental circular dichroism spectra. It should be added that structural data obtained from solution X-ray scattering in ref 53 agree with that crystal structure. Another argument against the assumption that exciton coupling could be responsible for the color tuning can be deduced from recent crystal structures of unbound astaxanthin, of several diacetates of astaxanthin, and of some related molecules.[54,55] All of these crystals have red or orange color, even though many different intermolecular orientations occur, and the distances are in some cases much smaller than in β-crustacyanin. None of the structures shows such a shift in the absorption spectrum that is large enough to turn the color of the crystals to blue.

6. DISCUSSION AND CONCLUSIONS

In this work, we reinvestigated several possible mechanisms for the bathochromic shift of AXT in crustacyanin by means of quantum chemical calculations of absorption, circular dichroism, and nuclear magnetic resonance spectra. Several conclusions can be drawn from our calculations, which will be discussed below in the context of earlier theoretical and experimental work.

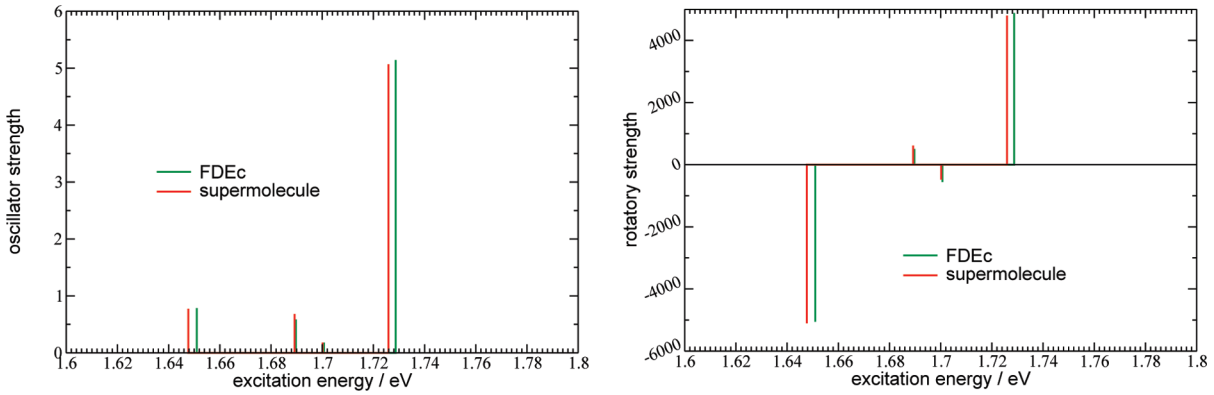

Figure 5. Stick representation of the absorption (left) and circular dichroism spectrum (right; SAOP/DZP) of the astaxanthin dimer from supermolecular (super) and FDEc calculations. Rotatory strengths are given in units of 10^{-40} esu^2·cm^2.

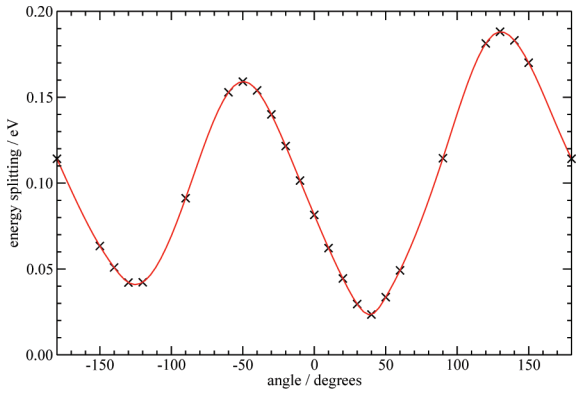

Figure 6. Excitonic splittings between the lowest and the highest of the four low-energy excited states of the astaxanthin dimer for different rotation angles. The angle measures the displacement from the crystal structure by a rotation around the axis indicated in Figure 4. Calculated data points are marked by crosses; the red line is a cubic spline interpolation to the data points.

Concerning the structural change from *s-cis* (solution) to *s-trans* (protein), we find a red-shift effect of 0.04 eV for the optimized *s-trans* structure, which increases to about 0.1 eV if we consider AXT in the crystal-structure geometry found in β-crustacyanin. The latter value is in line with former findings in refs 1 (0.12 eV) and 5 (0.09−0.13 eV, depending on the precise method/basis set used). It also fits the observed difference in the absorption maxima between canthaxanthin, which is related to the *s-cis* structure of astaxanthin, and rhodoxanthin, which is in a similar way related to *s-trans* astaxanthin. This difference amounts to 0.11 eV (482 nm vs 503 nm) in benzene and 0.12 eV (490 nm vs 514 nm) in DMSO.[56]

As far as the local environment is concerned, we have shown that the effect of the hydrophilic residues in the astaxanthin binding pocket in β-crustacyanin on the low-lying, bright B_u-like state is small. That does not necessarily mean that there is no general dielectric effect of the environment. In contrast, already the large differences in absorption energy in different solvents indicate that astaxanthin (as carotenoids in general) reacts quite sensitive to changes in the environment, e.g., it is well known that absorption bands of rhodopin glucoside and spheroidene decrease in energy by about 0.1 eV between *n*-hexane solution and the light-harvesting complex 2 (LH2) of *Rhodopseudomonas acidophila* and *Rhodobacter spheroides*, respectivley.[57] For carotenoids that contain conjugated keto groups, these shifts can be even larger, and it has been reported that even the mutation of a single amino acid can have a significant effect on the carotenoid absorption spectrum.[58] Furthermore, an intermolecular charge-transfer state has been invoked in a possible explanation for (part of) the protein-induced red shift of a keto-group-containing carotenoid in ref 59.

Several tests have been carried out in our work here to investigate the effect of a protonated histidine residue. The resulting changes are typically quite low, in particular if the shift in the absorption maximum of the superimposed absorption peaks in the spectrum is considered instead of just the lowest electronic transition with considerable HOMO−LUMO transition character. A first set of results was obtained on the basis of the SAOP exchange-correlation potential in TDDFT calculations. They were backed up by calculations with several other methods, including the CIS method. In ref 12 it has been shown that CIS can accurately predict the changes in the lowest B_u-like excitation energy caused by protonation, even though absolute excitation energies are considerably too high. However, even CIS only indicates a shift of −0.125 eV induced by the protonated histidine. These findings put some doubt on the explanation of the spectral shift mainly as a polarization effect of the surrounding protein, even if protonated histidine residues are assumed in the binding pocket. If no protonation is assumed, these polarization effects are, according to our calculations, even smaller. In the study in ref 1 it was concluded that such a protonation is not compatible with the NMR data for AXT in crustacyanin. Here, we analyzed this point on the basis of theoretical chemical shift differences between AXT and AXT with a protonated histidine residue. The resulting data are incompatible with the experimental counterpart, thus providing further evidence for neutral histidine residues in the binding pocket.

To analyze the third proposed color-tuning mechanism, we investigated the effect of exciton coupling on the absorption and circular dichroism spectra, rather than the splitting energies alone. We confirmed the data by Strambi and Durbeej[4] for the splitting energy, but we show in addition that the spectral distribution leads to a *blue shift* of the most intense exciton peak for this orientation rather than a red shift. However, the total effect on the superimposed spectrum is quite small. The fact that exciton couplings do not have a significant effect on the

absorption spectra of astaxanthin is corroborated by the red or orange color of crystals of unbound AXT, which is similar to the color of free AXT in solution.[54,55] Our calculations are qualitatively in line with the couplet signature in the experimental CD spectrum. A possible explanation for the larger exciton splitting estimated from the CD spectrum may be a slightly different inclination angle of the two chromophores.

In summary, it appears that none of the three major effects (conformational changes, polarization by the binding pocket, exciton splitting) can be responsible for the large bathochromic shift alone. However, on-site effects of 0.1−0.2 eV in proteins are not unusual for carotenoids with conjugated keto groups, and if conformational effects of about 0.1 eV are considered in addition, a large portion of the shift could be explained. Further investigations on the long-range electrostatic effect of the protein backbone or vibrational effects are necessary to make more definite conclusions on this dramatic color change.

■ ASSOCIATED CONTENT

Supporting Information. Additional figures and tables containing the optimized structures of *s-cis*- and *s-trans*-AXT, the energy of the absorption maximum obtained as a superposition of the four lowest excited states of the coupled AXT dimer for different distortion angles from the crystal structure, and data on the basis-set dependence of the exciton splitting in the AXT dimer are provided. This material is available free of charge via the Internet at http://pubs.acs.org.

■ AUTHOR INFORMATION

Corresponding Author

*E-mail: (J.N.) j.neugebauer@chem.leidenuniv.nl; (F.B.) f.buda@chem.leidenuniv.nl.

■ ACKNOWLEDGMENT

We thank Johan Lugtenburg for useful discussions. J.N. is supported by a VIDI grant (700.59.422) of The Netherlands Organization for Scientific Research (NWO). The use of supercomputer facilities was sponsored by The Netherlands National Computing Facilities (NCF), with support from NWO.

■ REFERENCES

(1) van Wijk, A. A. C.; Spaans, A.; Uzunbajakava, N.; Otto, C.; de Groot, H. J. M.; Lugtenburg, J.; Buda, F. *J. Am. Chem. Soc.* **2005**, *127*, 1438.
(2) Ilagan, R. P.; Christensen, R. L.; Chapp, T. W.; Gibson, G. N.; Pascher, T.; Polvka, T.; Frank, H. A. *J. Phys. Chem. A* **2005**, *109*, 3120.
(3) Buchwald, M.; Jencks, W. P. *Biochemistry* **1968**, *7*, 834.
(4) Strambi, A.; Durbeej, B. *J. Phys. Chem. B* **2009**, *113*, 5311.
(5) Durbeej, B.; Eriksson, L. A. *Phys. Chem. Chem. Phys.* **2004**, *6*, 4190.
(6) Durbeej, B.; Eriksson, L. A. *Phys. Chem. Chem. Phys.* **2006**, *8*, 4053.
(7) Buchwald, M.; Jencks, W. P. *Biochemistry* **1968**, *7*, 844.
(8) Britton, G.; Weesie, R. J.; Askin, D.; Warburton, J. D.; Gallardo-Guerrero, L.; Jansen, F. J.; de Groot, H. J. M.; Lugtenburg, J.; Cornard, J.-P.; Merlin, J.-C. *Pure Appl. Chem.* **1997**, *69*, 2075.
(9) Cianci, M.; Rizkallah, P. J.; Olczak, A.; Raftery, J.; Chayen, N. E.; Zagalsky, P. F.; Helliwell, J. R. *Proc. Natl. Acad. Sci. U.S.A.* **2002**, *99*, 9795.
(10) Shone, C. C.; Britton, G.; Goodwin, T. W. *Comp. Biochem. Physiol.* **1979**, *62B*, 507.
(11) Polívka, T.; Frank, H. A.; Enriquez, M. M.; Niedzwiedzki, D. M.; Liaaen-Jensen, S.; Helliwell, J. R.; Helliwell, M. *J. Phys. Chem. B* **2010**, *114*, 8760.
(12) Durbeej, B.; Eriksson, L. A. *Chem. Phys. Lett.* **2003**, *375*, 30.
(13) Kildahl-Andersen, G.; Lutnaes, B. F.; Liaaen-Jensen, S. *Org. Biomol. Chem.* **2004**, *2*, 489.
(14) Salares, V. R.; Young, N. M.; Bernstein, H. J.; Carey, P. R. *Biochim. Biophys. Acta* **1979**, *576*, 176.
(15) Wanko, M.; Hoffmann, M.; Strodel, P.; Koslowski, A.; Thiel, W.; Neese, F.; Frauenheim, T.; Elstner, M. *J. Phys. Chem. B* **2005**, *106*, 3606.
(16) *Amsterdam density functional program*; Theoretical Chemistry, Vrije Universiteit: Amsterdam, 2008; URL: http://www.scm.com.
(17) te Velde, G.; Bickelhaupt, F. M.; Baerends, E. J.; van Gisbergen, S. J. A.; Fonseca Guerra, C.; Snijders, J. G.; Ziegler, T. *J. Comput. Chem.* **2001**, *22*, 931.
(18) Becke, A. D. *Phys. Rev. A* **1988**, *38*, 3098.
(19) Perdew, J. P. *Phys. Rev. B* **1986**, *33*, 8822.
(20) Schipper, P. R. T.; Gritsenko, O. V.; van Gisbergen, S. J. A.; Baerends, E. J. *J. Chem. Phys.* **2000**, *112*, 1344.
(21) Gritsenko, O. V.; Schipper, P. R. T.; Baerends, E. J. *Chem. Phys. Let.* **1999**, *302*, 199.
(22) Gritsenko, O. V.; Schipper, P. R. T.; Baerends, E. J. *Int. J. Quantum Chem.* **2000**, *76*, 407.
(23) Zhao, Y.; Truhlar, D. G. *J. Phys. Chem. A* **2006**, *110*, 13126.
(24) Lee, C.; Yang, W.; Parr, R. G. *Phys. Rev. B* **1988**, *37*, 785.
(25) Becke, A. D. *J. Chem. Phys.* **1993**, *98*, 5648.
(26) Stephens, P. J.; Devlin, F. J.; Chabalowski, C. F.; Frisch, M. J. *J. Phys. Chem.* **1994**, *98*, 11623.
(27) Ahlrichs, R.; Bär, M.; Häser, M.; Horn, H.; Kölmel, C. *Chem. Phys. Lett.* **1989**, *162*, 165.
(28) Ridley, J.; Zerner, M. *Theor. Chim. Acta* **1973**, *32*, 111.
(29) Neese, F. *Orca 2.6, an ab initio, density functional and SCF-MO package*; Universität Bonn: Bonn, 2008; http://www.thch.uni-bonn.de/tc/orca.
(30) Neugebauer, J. *J. Chem. Phys.* **2007**, *126*, 134116.
(31) Neugebauer, J. *J. Phys. Chem. B* **2008**, *112*, 2207.
(32) Wesolowski, T. A.; Warshel, A. *J. Phys. Chem.* **1993**, *97*, 8050.
(33) Jacob, C. R.; Neugebauer, J.; Visscher, L. *J. Comput. Chem.* **2008**, *29*, 1011.
(34) Dulak, M.; Wesolowski, T. A. *J. Chem. Phys.* **2006**, *124*, 164101.
(35) Wesolowski, T.; Muller, R. P.; Warshel, A. *J. Phys. Chem.* **1996**, *100*, 15444.
(36) Perdew, J. P. In *Electronic Structure of Solids*; Ziesche, P., Eschrig, H., Eds.; Akademie Verlag: Berlin, 1991; p 11.
(37) Lembarki, A.; Chermette, H. *Phys. Rev. A* **1994**, *50*, 5328.
(38) Thomas, L. A. *Proc. Cambridge Philos. Soc.* **1927**, *23*, 542.
(39) Fermi, E. *Z. Phys.* **1928**, *48*, 73.
(40) Wesolowski, T. A.; Chermette, H.; Weber, J. *J. Chem. Phys.* **1996**, *105*, 9182.
(41) Wesolowski, T. A. *J. Am. Chem. Soc.* **2004**, *126*, 11444.
(42) Hsu, C.-P.; Hirata, S.; Head-Gordon, M. *J. Phys. Chem. A* **2001**, *105*, 451.
(43) Maitra, N. T.; Zhang, F.; Cave, R. J.; Burke, K. *J. Chem. Phys.* **2004**, *120*, 5932.
(44) Cave, R. J.; Zhang, F.; Maitra, N. T.; Burke, K. *Chem. Phys. Lett.* **2004**, *389*, 39.
(45) Starcke, J. H.; Wormit, M.; Schirmer, J.; Dreuw, A. *Chem. Phys.* **2006**, *329*, 39.
(46) Mazur, G.; Włodarczyk, R. *J. Comput. Chem.* **2009**, *30*, 811.
(47) Rinkevicius, Z.; Vahtras, O.; Ågren, H. *J. Chem. Phys.* **2010**, *133*, 114104.
(48) Send, R.; Sundholm, D.; Johansson, M. P.; Pawlowski, F. *J. Chem. Theory Comput.* **2009**, *5*, 2401.
(49) Shao, Y.; Head-Gordon, M.; Krylov, A. I. *J. Chem. Phys.* **2003**, *118*, 4807.
(50) Wang, F.; Ziegler, T. *J. Chem. Phys.* **2004**, *121*, 12191.
(51) Wang, F.; Ziegler, T. *J. Chem. Phys.* **2005**, *121*, 074109.

(52) Neugebauer, J. *ChemPhysChem* **2009**, *10*, 3148.
(53) Chayen, N. E.; Cianci, M.; Grossmann, J. G.; Habash, J.; Helliwell, J. R.; Nneji, G. A.; Raftery, J.; Rizkallah, P. J.; Zagalsky, P. F. *Acta Crystallogr., Sect. D* **2003**, *59*, 2072.
(54) Bartalucci, G.; Coppin, J.; Fischer, S.; Hall, G.; Helliwell, J. R.; Helliwell, M.; Liaaen-Jensen, S. *Acta Crystallogr., Sect. B* **2007**, *63*, 328.
(55) Bartalucci, G.; Fischer, S.; Hall, G.; Helliwell, J. R.; Helliwell, M.; Liaaen-Jensen, S.; Warren, J. E.; Wilkinson, J. *Acta Crystallogr., Sect. B* **2009**, *65*, 238.
(56) Chábera, P.; Fuciman, M.; Hříbek, P.; Polívka, T. *Phys. Chem. Chem. Phys.* **2009**, *11*, 8795.
(57) Polívka, T.; Zigmantas, D.; Herek, J.; He, Z.; Pascher, T.; Pullerits, T.; Cogdell, R.; Frank, H.; Sundstrom, V. *J. Phys. Chem. B* **2002**, *106*, 11016.
(58) Schulte, T.; Niedzwiedzki, D. M.; Birge, R. R.; Polívka, T.; Hofmann, E.; Frank, H. A. *Proc. Natl. Acad. Sci. U.S.A.* **2009**, *106*, 20764.
(59) Polívka, T.; Kerfeld, C. A.; Pascher, T.; Sundström, V. *Biochemistry* **2005**, *44*, 3994.
(60) Humphrey, W.; Dalke, A.; Schulten, K. *J. Mol. Graphics* **1996**, *14.1*, 33.
(61) Schreiber, M.; Silva-Junior, M. R.; Sauer, S. P.; Thiel, W. *J. Chem. Phys.* **2008**, *128*, 134110.
(62) Leopold, D. G.; Pendley, R. D.; Roebber, J. L.; Hemley, R. J.; Vaida, V. *J. Chem. Phys.* **1984**, *81*, 4218.
(63) D'Amico, K. L.; Manos, C.; Christensen, R. L. *J. Am. Chem. Soc.* **1980**, *102*, 1777.